Distinct subdomain organization and molecular composition of a tight junction with adherens junction features

Fabio D. Nunes[1,*], Lanier N. Lopez[1,*], Harrison W. Lin[1,*], Caroline Davies[1], Ricardo B. Azevedo[1], Alexander Gow[2,‡] and Bechara Kachar[1,‡]

[1]Laboratory of Cellular Biology, National Institute on Deafness and Other Communication Disorders, National Institutes of Health, Bethesda, MD 20892, USA
[2]Center for Molecular Medicine and Genetics, Carman and Ann Adams Dept of Pediatrics, Dept of Neurology, Wayne State University School of Medicine, Detroit, MI 48201, USA

*These authors contributed equally to this manuscript
‡Authors for correspondence (e-mail: agow@med.wayne.edu; kacharb@nidcd.nih.gov)

Accepted 29 August 2006
Journal of Cell Science 119, 4819-4827 Published by The Company of Biologists 2006
doi:10.1242/jcs.03233

Summary

Most polarized epithelia constrain solute diffusion between luminal and interstitial compartments using tight junctions and generate mechanical strength using adherens junctions. These intercellular junctions are typically portrayed as incongruent macromolecular complexes with distinct protein components. Herein, we delineate the molecular composition and subdomain architecture of an intercellular junction between sensory and non-sensory cells of the inner ear. In this junction, claudins partition into claudin-14 and claudin-9/6 subdomains that are distinguishable by strand morphology, which contrasts with in vitro data that most claudins co-assemble into heteromeric strands. Surprisingly, canonical adherens junction proteins (p120ctn, α- and β-catenins) colocalize with the claudin-9/6 subdomain and recruit a dense cytoskeletal network. We also find that catenins colocalize with claudin-9 and claudin-6, but not claudin-14, in a heterologous system. Together, our data demonstrate that canonical tight junction and adherens junction proteins can be recruited to a single junction in which claudins partition into subdomains and form a novel hybrid tight junction with adherens junction organization.

Supplementary material available online at
http://jcs.biologists.org/cgi/content/full/119/23/4819/DC1

Key words: Apical junctional complex, Outer hair cell, Reticular lamina, Organ of Corti, Tight-adherens junction, Cochlea

Introduction

The capacity of cells to establish permeability barriers between compartments of differing solute compositions has enabled organisms to evolve and thrive in a multicellular state, resistant to adverse environmental changes. In most cell types, the unit of function is the apical junctional complex (AJC) comprised of tight junctions (TJs) that serve as solute permeability barriers, and adherens junctions (AJs) that serve an adhesive role to maintain tissue integrity against mechanical stress (Aijaz et al., 2006; Farquhar and Palade, 1963; Jahnke, 1975).

Claudins constitute the major diffusion barrier of TJs (Furuse et al., 1998; Gow et al., 1999) and together with occludin, zonula occludens (ZO) family members and other cytoplasmic proteins generate apical and basolateral domains in the plasma membrane to maintain cell polarity (Schneeberger and Lynch, 2004; Tsukita et al., 2001). Cadherins constitute the major adhesive component of AJs and recruit $p120^{ctn}$, α- and β-catenins and the cytoskeleton to the plasma membrane while forming homophilic and heterophilic interactions between adjacent cells to generate a structural framework for the entire cell sheet (Gumbiner, 2005; Nagafuchi, 2001; Tsukita et al., 2001). Adherens junctions are porous in mammals and play no role as a diffusion barrier.

The TJs and AJs that usually comprise AJCs are widely thought to consist of distinct and largely non-overlapping sets of proteins; however, recent studies in invertebrates challenge this view. For example, the *C. elegans* regulatory protein VAB-9, which is a member of the PMP22/EMP/Claudin family, regulates adhesion at AJs via interactions with invertebrate orthologs of a cadherin-catenin complex (Simske et al., 2003).

In the inner ear, intercellular junctions harboring multiple claudins are widespread and essential for normal hearing (Ben-Yosef et al., 2003; Kitajiri et al., 2004; Wilcox et al., 2001), with most cells assembling canonical AJCs that fulfill archetypal roles of occlusion and adhesion (Jahnke, 1975; Wilcox et al., 2001). By contrast, the interface between mechanosensory outer hair cells (OHCs) and their supporting Deiter cells (DCs) in the organ of Corti is a morphologically distinct unitary junction (Gulley and Reese, 1976; Jahnke, 1975). This large 3-5 μm junction is the only point of contact between OHCs and DCs and must be strongly adhesive and occluding to withstand the rigors of organ of Corti physiology, including: sound-induced resonance of the basilar membrane over a range of tens of kilohertz; vigorous movements associated with OHC electromotility, which generate shear and strain forces up to several nanoNewtons (Ospeck et al., 2003); a strong electrical gradient of ~100 mV; and a large K^+ gradient of ~150 mM (Ospeck et al., 2003; Wangemann et al., 1995).

Herein, we dissect the DC-OHC junction and localize proteins that are pivotal to junction formation and regulation. Claudin-14 is confined to a small apical subdomain whereas claudin-9 and -6 are enriched in a larger basal subdomain. Unexpectedly, AJ proteins $p120^{ctn}$, β-catenin and α-catenin localize to the claudin 9/6-rich domain and assemble an extensive actin cytoskeleton. Furthermore, we demonstrate in transfected COS-7 cells that claudin-9 and claudin-6, but not claudin-14, colocalize with catenins at sites of TJ assembly. Together, our data demonstrate extensive colocalization of TJ and AJ proteins in a functional junction in vivo, indicating that these proteins can be recruited in novel combinations to fulfill specific needs of the cell.

Results

Inner hair cells (IHCs) and OHCs in the cochlea are organized into four rows along the length of the organ of Corti with their apices embedded in a rigid transcellular plate called the reticular lamina (Fig. 1a). The reticular lamina is formed by the processes of supporting cells and its rigidity is conferred by well-developed cell-cell junctions between all cells as well as by an extensive cytoskeleton in supporting cells. Of particular interest are DCs, which contact the apices of OHCs and also anchor these cells from below to the basement membrane.

Intercellular junctions at cell-cell contacts in the reticular lamina

Viewed from above, the organization of DC rhomboidal phalanges in the reticular lamina is punctuated by the apices of OHCs. Four phalanges and one OHC are shown in color in Fig. 1b. The contribution to cell-cell contacts from DC-OHC heterotypic junctions (green) is greater than DC-DC homotypic junctions (red), with a length ratio of approximately 6:1, indicating that DC-OHC junctions predominate. Tight appositions between OHCs (white asterisk in Fig. 1c) and adjacent DC phalanges (white arrows) are critical to reticular lamina integrity.

Fig. 1d shows the morphologies of DC-DC and DC-OHC junctions. DC-DC junctions comprise TJs and AJs in canonical AJCs. DC-OHC junctions are distinct (Fig. 1e-g) but share two important features with DC-DC junctions. First, the very close contact between the membranes in the DC-OHC junctions is similar to that in DC-DC TJs. Second, the cytoplasmic plaque in DC-OHC junctions is highly developed, except for the extreme apical region where the plaque is small, and similar to DC-DC AJs. Unlike DC-DC AJCs, a single DC-OHC junction spans the entire thickness of the reticular lamina.

Freeze-etching of a DC-OHC junction

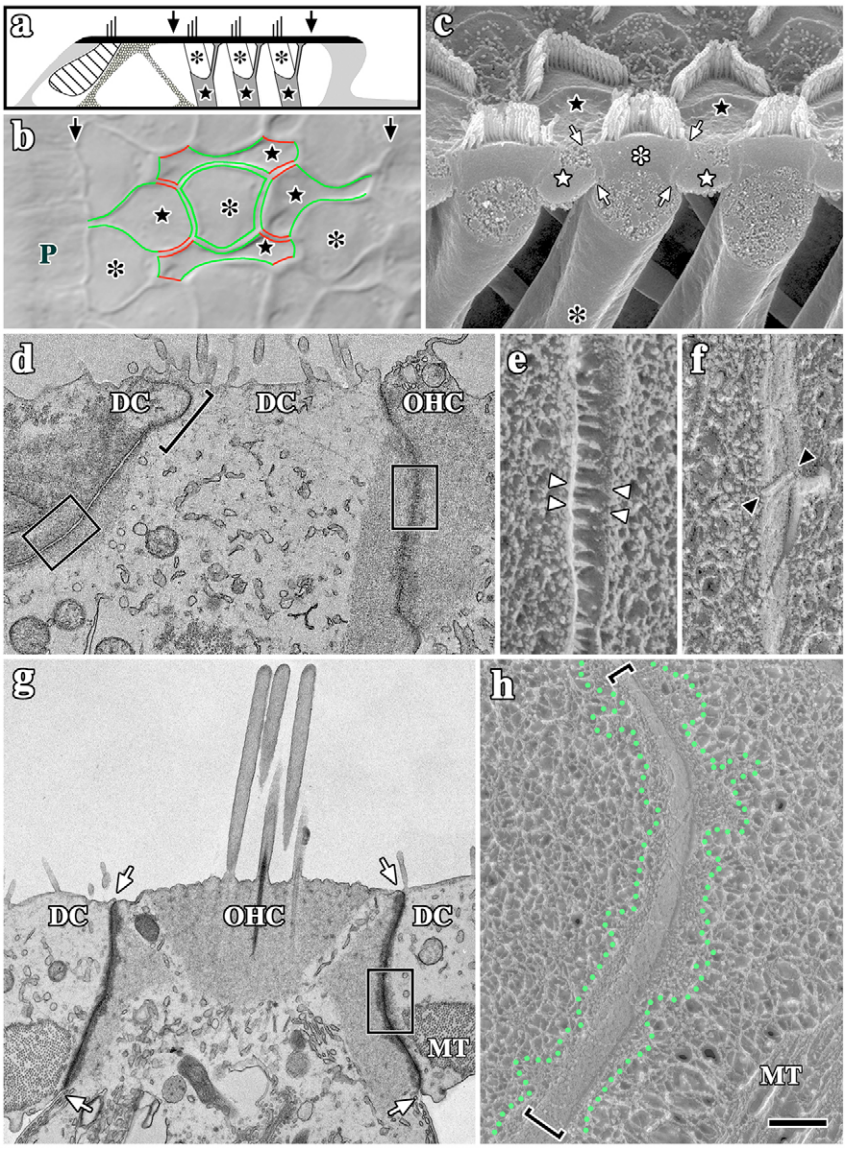

Fig. 1. Morphological features of the novel DC-OHC heterotypic junction. (a) Organ of Corti schematic. Pillar Cells (stippled) separate IHC (hatching) from OHC (black asterisks). Vertical black arrows, reticular lamina. (b) DIC micrograph of the reticular lamina apical surface. Green, DC-OHC junctions; red, DC-DC junctions. P, pillar cells. (c) SEM of the apical surface and vertical cut away of the reticular lamina. (d) TEM of two DC phalanges (left and center) and an OHC (right) reveals the morphologies of DC-DC and DC-OHC junctions. Square brackets, TJ in the DC-DC AJC. (e) Freeze-etching of a DC-DC AJ (left rectangle in d) reveals fibrils across the intercellular space (white arrowheads) likely corresponding to E-cadherin cross-bridges. (f) Freeze-etching of a DC-OHC junction (right rectangle in d) reveals fibrils in a DC-OHC junction (black arrowheads) similar to those in conventional freeze-fracture replicas (Fig. 5). (g) TEM of an OHC flanked by DCs shows DC-OHC junction morphology. (h) Freeze-etching reveals a DC-OHC junction (rectangle in g). The plasma membranes (brackets) are flanked by a dense cytoplasmic protein coat (green dots) and a large actin cytoskeleton. Tissue samples from: guinea pig, (b,e-h); rat (d) and mouse (c). Black stars, DC phalanges; white arrows, DC-OHC interface; white asterisks, apices of OHCs; MT, microtubule bundle. Bar in h, 7.6 μm (b); 6.4 μm (c); 0.6 μm (d); 0.1 μm (e,f); 0.85 μm (g); 0.3 μm (h).

(rectangle in Fig. 1g) reveals important aspects of heterotypic junctions (Fig. 1h). Square brackets delineate juxtaposed DC-OHC plasma membranes exposed by the fracture plane. Flanking these membranes are dense protein coats (inside the green dotted lines) that spawn extensive cytoskeletal networks extending beyond the field of view. Such a high degree of organization is common in AJs but most unusual in TJs.

Tight junction proteins are recruited to heterotypic junctions

To begin a molecular dissection of DC-OHC junctions, we analyzed a database of 25,000 randomly sequenced cDNAs from a non-amplified, non-subtracted mouse organ of Corti expression library (Pompeia et al., 2004). Seven *Claudin* genes are represented; however, *Claudin-9* is by far the predominant family member; nine clones encoding claudin-9 were sequenced from the library and one clone for each of claudin-3, -5, -6, -8, -11 and -14. Other claudins may also be expressed at low levels in the cochlea and not detected in our library analysis. Indeed Claudin-1, -2, -7, -13 and -18 have been detected by immunocytochemical analyses (Kitajiri et al., 2004).

To locate TJs in the reticular lamina, we labeled organ of Corti whole-mount preparations with antibodies against ZO-1 (Fig. 2a) and occludin (data not shown). Confocal micrographs reveal both proteins in all heterotypic and homotypic junctions as are claudin-9 and -6 (Fig. 2b,c, respectively). We consistently find that the intensity of fluorescence labeling of DC-DC junctions exceeds that of DC-OHC junctions for most antibodies. While we cannot rule out the possibility that heterotypic junctions may contain lower levels of TJ and AJ proteins, a more likely explanation is that the greater density of cytoplasmic plaque proteins along TAJs interferes with antibodies binding to their epitopes. Thus, the colocalization of these proteins, and morphological evidence (Fig. 1), indicates that DC-OHC junctions are TJs.

Immunoelectron micrographs reveal the locations of ZO-1, occludin and claudin-9 and -6 in rat, guinea pig and mouse reticular laminae (Fig. 2e-j). These micrographs are representatives from more than ten DC-OHC junctions labeled with each antibody. Occludin, ZO-1, and claudin-9 are abundant proteins present throughout DC-OHC junctions. Claudin-6 labeling is observed at much lower levels and in central regions of the junctions (Fig. 2i,j).

Claudin-14 is restricted to an apical subdomain in heterotypic junctions

In contrast to claudin-9 and -6, the distribution of claudin-14 is preferentially localized to heterotypic junctions (Fig. 2d,o) and, specifically, to the apical-most region of DC-OHC contacts. Indeed, the confocal micrograph in Fig. 2o is a single optical section near the apical surface of the reticular lamina showing all DC-DC and DC-OHC junctions labeled with anti-ZO-1 antibodies (blue) and claudin-14 colocalization only in DC-OHC junctions (green).

Five representatives of this asymmetry are shown in Fig. 2k-n,p from more than ten junctions examined for each of the two claudin-14 antibodies used (PB196 and PB321). Thus, not only can claudins be preferentially targeted to specific TJs within a single cell but also to specific subdomains in a single TJ. Fig. 2p shows a wide view of the DC-OHC junctions to demonstrate the absence of non-specific antibody binding associated with the PB 321 anti-claudin-14 antibody. Currently, we are unable to ascertain the identity of the intercellular binding partner of claudin-14 in the juxtaposed DC membranes.

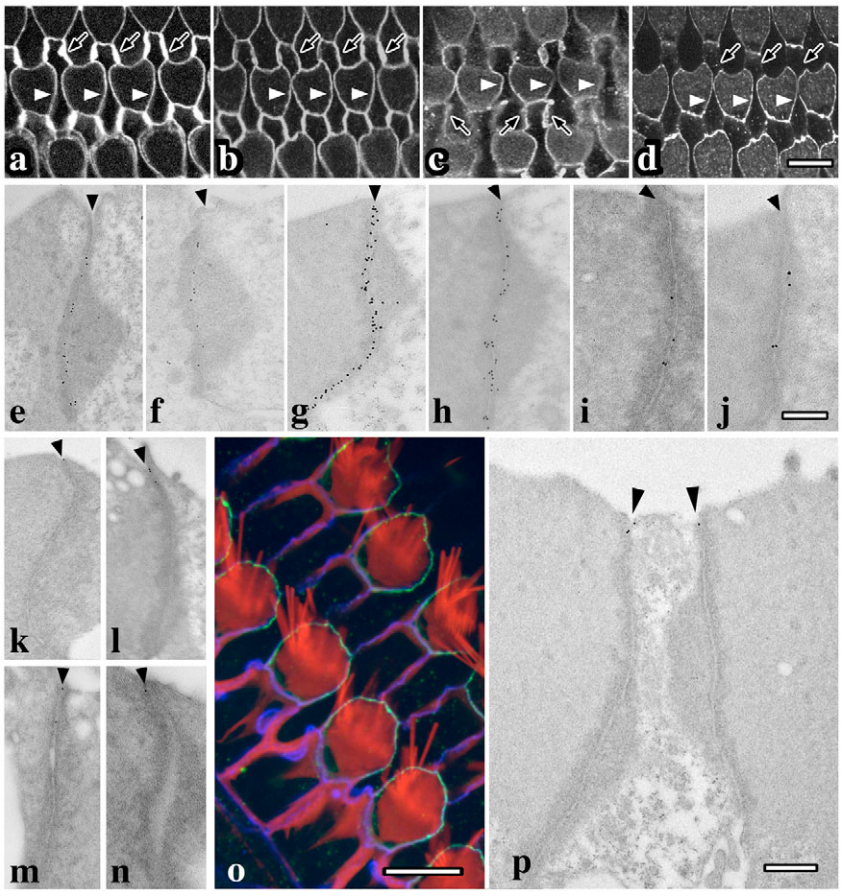

Fig. 2. Immunolocalization of TJ proteins in the reticular lamina. (a-d) Immunofluorescence labeling of the reticular lamina for ZO-1 (a), claudin-9 (b), claudin-6 (c) and claudin-14, with the antibody PB196 (d) at DC-OHC (white arrowheads) and DC-DC junctions (black arrows). (e-n) Immunogold electron microscopy gold labeling of DC-OHC junctions showing ZO-1 (e), occludin (f), claudin-9 (g,h), claudin-6 (i,j) and claudin-14, with the antibody PB196 (k-n). OHCs are to the right. Black arrowheads, apices of junctions. (o) Single confocal optical section near the apical surface of the reticular lamina showing immunofluorescence for claudin 14 (with the antibody PB321) in DC-OHC junctions (green), ZO-1 in DC-DC and DC-OHC junctions (blue) and actin (labeled with rhodamine phalloidin) in DC-DC and DC-OHC junctions and stereocilia. (p) Immunogold electron microscopy of claudin 14 labeling (with the antibody PB321) of DC-OHC junctions (arrowheads). The absence of background away from the junctions attests to the specificity of antibody labeling. Tissue samples from: guinea pig, (a-f,o,p); rat (g,i,k,l) or mouse (h,j,m,n). Bar in d, 10 μm (a-d); 0.4 μm (e-n); 10 μm (o); 0.3 μm (p).

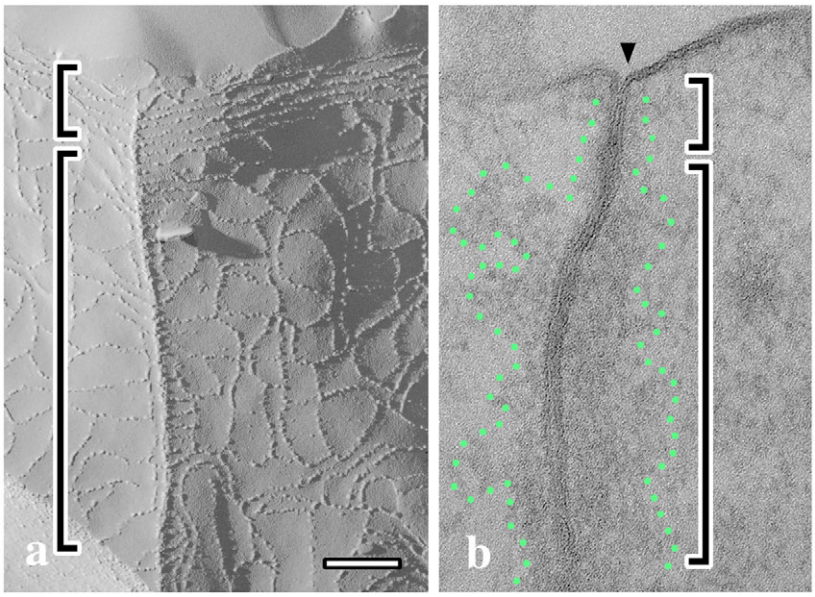

Fig. 3. Ultrastructure of the DC-OHC junction. (a) Freeze fracture shows the organization of intramembranous fibrils in two subdomains (brackets) of a DC-OHC junction at a tricellular DC-OHC-DC interface. (b) Electron micrograph from a 30 nm thin section shows the actin cytoskeleton (green dots) at a DC-OHC junction. Two subdomains (brackets) are apparent. Bar, 0.34 μm.

In freeze fracture replicas, DC-OHC junctions exhibit an extensive and complex intramembranous fibril morphology that justifies the TJ epithet. The junction can be divided into two broad regions (square brackets in Fig. 3a, supplementary material Fig. S1); the apical region (upper bracket) is characterized by closely-spaced mainly parallel intramembranous fibrils, while the more extensive subjacent region is comprised of mainly meandering fibrils (lower bracket). Such a striking dichotomy in fibril organization contrasts with the archetypal view of TJs where claudins copolymerize relatively uniformly into fibrils (Furuse et al., 1999; Tsukita et al., 2000).

Additional features of the subdomain organization of DC-OHC junctions are revealed in 30 nm sections cut perpendicular to the membrane. Fig. 3b shows partitioning of the cytoplasmic plaque into two regions (square brackets). The green dotted lines delineate the boundary between the plaque and the cytoplasm. In the apical-most region (upper bracket), the plaque is small and typical of TJs in AJCs. Interestingly, this region corresponds to the parallel intramembranous fibrils observed in freeze fracture replicas (Fig. 3a), which in turn correspond to the anti-claudin-14 labeled region in Fig. 2k-n,p. Subjacent to this subdomain (lower bracket), the plaque is well-developed and is comparable to AJs in AJCs. This region corresponds to the claudin-9 and -6 containing region (Fig. 2g-j).

Adherens junction proteins and β-actin are recruited to heterotypic junctions

In Fig. 2 and Fig. 3a, we demonstrate that DC-OHC junctions are TJs; however, Fig. 1f,h and Fig. 3b raise issues that call into doubt the distinctions between TJs and AJs. For example, how is an extensive actin cytoskeleton recruited to these TJ strands and how is this relationship maintained? Tight junctions are not normally associated with an extensive cytoskeleton, and this view is borne out in Fig. 1d. To address these issues, we examined heterotypic junctions for the presence of proteins that are critical for actin cytoskeleton recruitment at AJCs.

First, we labeled the organ of Corti with anti-β-catenin antibodies. β-catenin is known to recruit α-catenin and formins to AJCs, which nucleate actin polymerization (Kobielak et al., 2004; Zigmond, 2004). Confocal micrographs (Fig. 4a) show strong labeling of the AJs at DC-DC junctions (Fig. 1d); however, the perimeters of OHCs are also labeled, indicating that β-catenin is recruited to heterotypic junctions. Indeed, immunoelectron micrographs (Fig. 4b) confirm the presence of β-catenin at DC-OHC contacts. Importantly, the extreme apical region of the junction is unlabeled; this is the claudin-14-rich, cytoskeleton-poor region. We find that α-catenin is also recruited to these junctions (data not shown) and coincident with β-catenin, indicating the assembly of a macromolecular complex that recruits the cytoskeleton.

Second, we labeled the organ of Corti with anti-p120^{ctn} antibodies, which is another catenin family member that regulates protein turnover at AJs (Peifer and Yap, 2003). Again, homotypic and heterotypic junctions (Fig. 4c) are labeled and the immunoelectron micrograph in Fig. 4d shows that p120^{ctn} is coincident with β-catenin and absent from the cytoskeleton-poor region. Thus, these data demonstrate that heterotypic junctions outside of the claudin-14-rich region recruit three AJ proteins and account for the presence of a well-developed cytoskeleton. Currently, we cannot exclude the possibility that p120^{ctn} and β-catenin are localized predominantly to the DC side of the heterotypic TJs.

Third, to determine if the actin cytoskeleton at heterotypic junctions is similar to that at AJs, we used anti-β-actin antibodies. Pillar cells, which separate IHCs and OHCs in the organ of Corti (P in Fig. 1a), assemble canonical AJCs and are heavily labeled for β-actin (Fig. 4e). In addition, anti-β-actin antibodies decorate DC-OHC junctions, excluding the extreme apical region (Fig. 4f), which corresponds with the distributions of p120^{ctn} and β- and α-catenins and suggests a functional complex. Together, the data in Figs 1-4 demonstrate that DC-OHC exhibits important characteristics of both TJs and AJs.

Finally, we labeled organ of Corti preparations with anti-E-, N- and P-cadherin antibodies to identify bone fide AJs and determine their spatial organization with respect to TJs. Fig. 4g reveals TJs and E-cadherin based AJs only between DC-DC contacts. Importantly, ZO-1 is recruited to the perimeter of OHCs; however, E-cadherin is absent from these sites. Furthermore, we are unable to detect N- and P-cadherins. Thus, AJ cytoplasmic proteins are recruited to DC-OHC junctions in the absence of classical cadherins. Currently, we cannot formally exclude the possibility that an unknown cadherin-like protein is localized at DC-OHC junctions. However, such a protein would have to function within the confines of TJ membrane appositions and intercalate into or between TJ strands. These features have not been demonstrated for

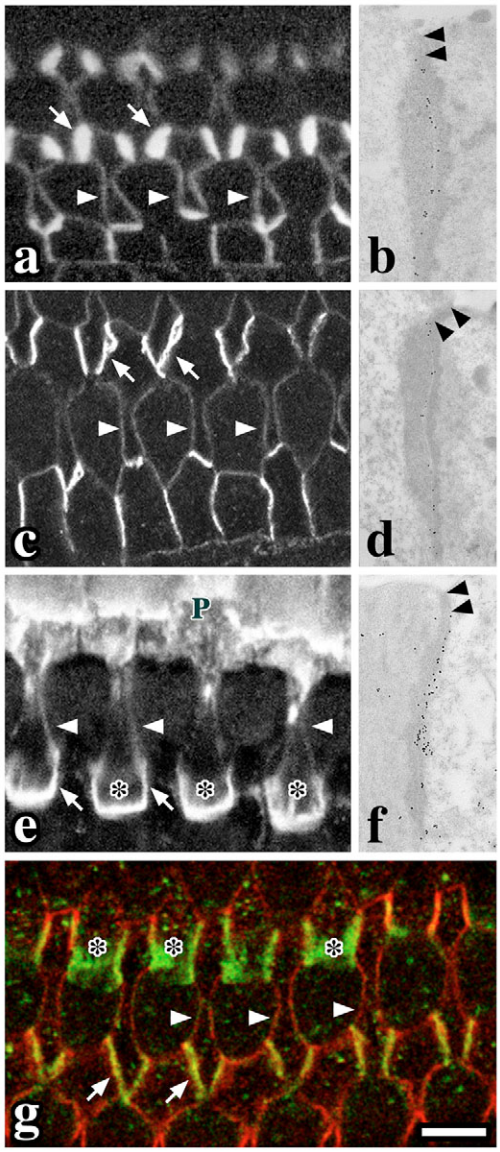

Fig. 4. Immunolocalization of AJ proteins in the reticular lamina. (a,c,e) Whole-mount preparations show β-catenin (a), p120^{ctn} (c) and β-actin (e) localized at DC-DC junctions (asterisks and arrows) and DC-OHC junctions (arrowheads). P in (e), pillar cells. (b,d,f) ImmunoEM shows β-catenin (b), p120^{ctn} (d) and β-actin (f) at DC-OHC junctions. OHCs are to the right. Black arrowheads, claudin-14-rich apical subdomain. (g) Whole-mount preparation shows E-cadherin (green) at DC-DC junctions (arrows and asterisks) and ZO-1 (red) at DC-DC (arrows) and DC-OHC junctions (arrowheads). Tissue samples are from guinea pig. Bar in g, 10 μm (a,c,e,g); 0.7 μm (b,d,f).

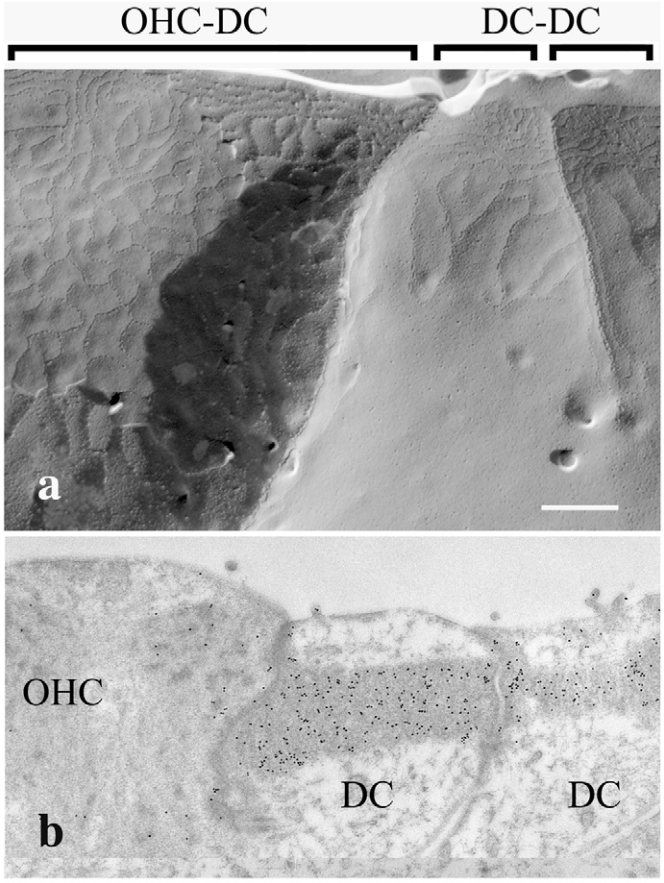

Fig. 5. Ultrastructure of the DC-OHC and DC-DC junctions. (a) Wide field freeze-fracture view of DC-OHC and DC-DC junctions reveals the overall organization of tight junction strands and the distinct morphologies between the DC-DC and DC-OHC junctions. (b) Anti-β-actin immunoEM of DC-OHC and DC-DC junctions showing the dense labeling of the cytoplasmic plaque. Importantly, the plane of section passes through the plaque (electron opaque band) revealing it to be a continuous band across the DC phalanges between DC-DC and DC-OHC junctions. Gold particles also label other components of the apical region of the OHC, which correspond to the actin-rich cuticular plate of these cells. Bar, 0.2 μm.

classical or protocadherins, which are known to form extended linear bridges between cells (Fig. 1e).

The cytoplasmic plaque forms a continuous band between DC-DC and DC-OHC junctions

In view of the similarities and differences we observe between DC-DC and DC-OHC junctions, we sought to determine if these cell-cell contacts are completely separable entities or if they form a continuum around the perimeter of each cell. The freeze-fracture replica in Fig. 5a shows the tight junction strands at a DC-OHC heterotypic junction (left) and two DC-DC homotypic junctions. The organization of strands is distinct in DC-DC and DC-OHC junctions. In Fig. 5b, immunogold electron microscopy using antibodies raised against β-actin shows that gold particles heavily decorate an electron dense band in DCs that is continuous between DC-DC and DC-OHC junctions. This band corresponds to the cytoplasmic plaque of the junctional complexes within these cells and demonstrates that intercellular junctions in the reticular lamina are continuous rather than discrete entities. Gold particles also label electron-dense areas of the apical region of the OHC, which correspond to the actin-rich cuticular plate of these cells.

Claudin-9 and claudin-6 colocalize with β-catenin and p120^{ctn} in heterologous cells

The presence of multiple catenins and a β-actin-containing cytoskeleton at DC-OHC junctions in the absence of cadherins suggests novel mechanisms for recruitment of plaque proteins

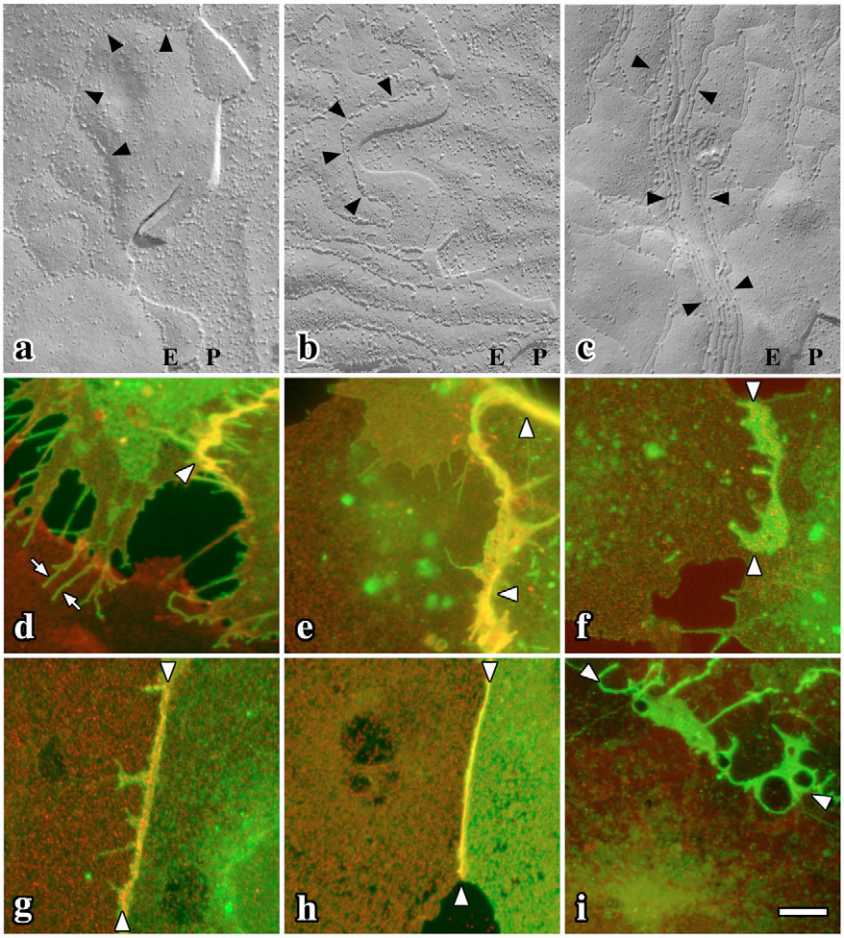

Fig. 6. Heterologous expression of claudins in transfected COS-7 cells. (a-c) Freeze fracture of unfixed transfected COS-7 cells shows fibrils (black arrowheads) for GFP-claudin-9 (a), -6 (b) and -14 (c) on the P- and E-fracture faces. (d-f) Confocal colocalization (white arrowheads) of endogenous β-catenin (red) with GFP-claudin-9 (d) and -6 (e) but not -14 (f) (green) at transfected cell-cell contacts. Arrows in (d), GFP-claudin-9 in filopodia of a transfected cell. (g-i) Confocal colocalization (white arrowheads) of endogenous $p120^{ctn}$ (red) and GFP-claudin-9 (d) and -6 (e) but not -14 (f) (green). Bar in i, 0.15 μm (a-c); 3.4 μm (d-i).

to cell-cell contacts. To determine if claudins can recruit catenins in heterologous systems, we expressed several GFP-claudin fusion proteins in COS-7 cells. COS-7 cells do not normally form tight junctions (supplementary material Fig. S2) and previously have been used for the heterologous expression of junctional proteins.

Freeze fracture replicas of COS-7 cell plasma membranes expressing GFP-claudin-9, -6 or -14 (Fig. 6) reveal intramembranous fibrils at cell-cell contacts. GFP-claudin-9 and -6 TJs (Fig. 6a,b) exhibit a meandering/anastomosing morphology similar to fibrils in vivo (Fig. 3a, lower bracket). GFP-claudin-14 fibrils (Fig. 6c) are predominantly parallel and compact and are similar to the apical-most region of DC-OHC junctions (Fig. 3a, upper bracket). Thus, these individual claudins autonomously govern strand morphology.

To determine if claudins can recruit regulatory AJ proteins, we labeled transfected COS-7 cells with anti-β-catenin antibodies. Yellow fluorescence at contact zones between two GFP-claudin-9 expressing cells (Fig. 6d) demonstrates that β-catenin is enriched at cell-cell contacts where TJs are assembled. Fig. 6e shows that GFP-claudin-6 shares the ability to associate with β-catenin. By contrast, GFP-claudin-14 cannot recruit β-catenin (Fig. 6f). In addition to β-catenin, COS-7 cells constitutively express $p120^{ctn}$ and we find that this protein is also recruited to TJs by GFP-claudin-9 and -6 (Fig. 6g,h), but not GFP-claudin-14 (Fig. 6i). Thus, we find that claudin-9 and -6, but not claudin-14, colocalize with AJ regulatory proteins in a heterologous system, but only at cell-cell contacts resulting in TJ strand formation. Importantly, these data accord with domain-specific recruitment of the cytoskeleton in DC-OHC junctions in vivo.

Discussion

In polarized epithelia, the paracellular space is defined and regulated by TJs and AJs, which exhibit distinct spatial, morphological and functional properties. These intercellular junctions utilize cohorts of structural and regulatory proteins that are thought to be largely non-overlapping. In the current study, we present morphological and functional evidence of a novel hybrid intercellular junction in the organ of Corti that, hitherto, has not been characterized in molecular detail but, nonetheless, appears to exhibit similar functional and molecular properties to apical junctions in at least some invertebrate species (Simske et al., 2003). This junction, which we designate a tight-adherens junction (TAJ), combines critical features of both TJs and AJs into a single large occluding junction. A schematic representation of the TAJ in Fig. 7 summarizes the locations of molecular components that we have identified and illustrates salient features of this hybrid junction for comparison with a canonical AJC.

Claudins segregate into morphologically- and spatially-defined subdomains

An intriguing and unexpected property of DC-OHC junctions is the presence of two subdomains of intramembranous fibrils with distinct morphologies. Previous studies in transfected fibroblasts indicate that claudins form heteromeric polymers in the plane of the bilayer and generate mixed TJ strands (Furuse et al., 1999); thus, it is surprising that claudin-14 is asymmetrically localized in heterotypic junctions. Nonetheless, we regard this confinement as a reflection of bona fide compartmentalization in TAJs for several reasons. First, the apical-most subdomain comprising parallel intramembranous fibrils (Fig. 3a) correlates with the localization of claudin-14 in immunoelectron micrographs (Fig. 2k-n,p). Second, transmission electron micrographs reveal two distinct subdomains of the cytoplasmic plaque (Fig. 3b) and, again, the apical-most subdomain corresponds to the claudin-14-enriched region. Finally, parallel strands in the claudin-14 subdomain resemble those in transfected COS-7

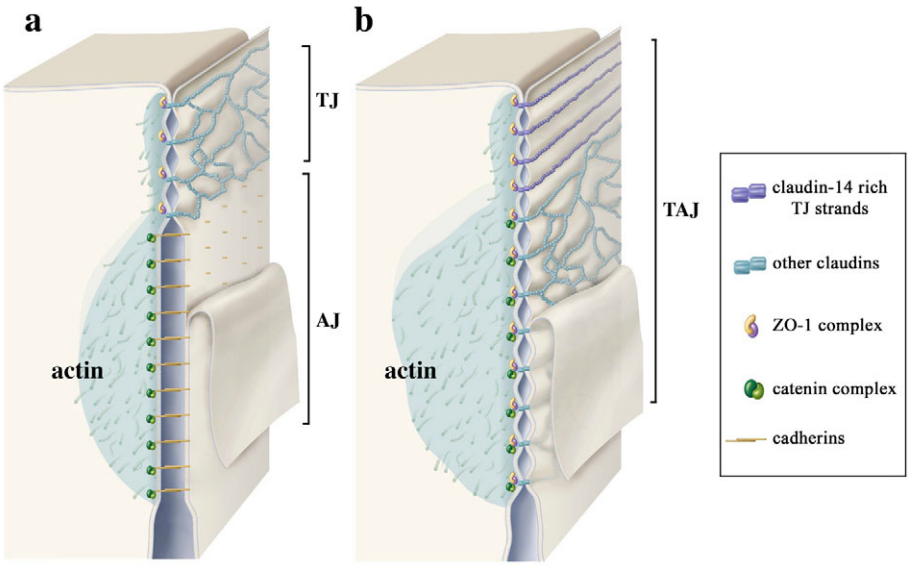

Fig. 7. Morphology, subdomain architecture and molecular components of AJCs and TAJs. (a) Diagram of a canonical AJC depicting a TJ and an AJ. The TJ comprises claudin-based anastomosing contacts between adjacent cell membranes. A ZO-1 scaffold assembles the underlying dense plaque and recruits a discrete actin cytoskeletal network. The AJ comprises a belt of cadherin-based transmembrane bridges and a catenin molecular complex assembles the underlying dense cytoplasmic plaque and recruits an extensive actin cytoskeletal network. (b) Diagram of a unitary, hybrid tight-adherens junction (TAJ) at the DC-OHC interface. The apical-most region of the TAJ is a claudin-14-rich subdomain of parallel TJ strands and the underlying ZO-1 scaffold assembles a small actin cytoskeletal network. A second subdomain enriched in claudin-9/6 forms an extensive belt of anastomosing membrane contacts. The underlying ZO-1 scaffold and the catenin molecular complex assemble a dense cytoplasmic plaque and recruit an extensive actin cytoskeletal network. The dense cytoplasmic plaque is localized to TAJs at a location that is analogous to their classical location in the canonical AJC.

cells expressing claudin-14 but not claudin-9 or -6 (Fig. 6a-c).

Currently, it is unclear whether mixed TJs exhibit combinatorial morphologies dependent on stoichiometric ratios of contributing claudins or if some claudins prevail over others. In the case of the apical-most region of DC-OHC junctions, claudin-14 appears to specify the parallel strand morphology although we cannot rule out the presence of other parallel strand-forming claudins synthesized by OHCs that may contribute to this morphology. Furthermore, we cannot rule out a role for the intercellular binding partner of claudin-14 synthesized by DCs. In this regard, our data in Fig. 2d,p and previous in situ data (Ben-Yosef et al., 2003) suggest that claudin-14 expression may be OHC-specific in the reticular lamina, which necessitates the involvement of an unknown claudin to form the strands between the DC and OHC cell membranes. In any case, asymmetry within TAJs and compartmentalization of claudins into distinct subdomains, with distinct architecture and molecular composition, provides a compelling explanation for deafness and OHC degeneration in *Claudin-14*-null mice (Ben-Yosef et al., 2003) and the absence of compensation by claudin-9 and -6 in these mutants.

The hybrid nature of DC-OHC junctions

Canonical TJs and AJs have been characterized extensively from many species and exhibit distinct features. First, the extracellular distance between plasma membranes of apposing cells is smaller for TJs than AJs. Second, the cytoplasmic plaque associated with TJs is smaller than AJs and the extent of the cytoskeleton recruited correlates with plaque density. Finally, TJs border the apical domain of the cell and AJs are spatially separated and subjacent.

Plasma membrane spacing at TAJs is typical of TJs and at least three claudins localize along its length. The dense cytoplasmic plaque is typical of AJs and we show that catenins, but not cadherins, are present and recruit an extensive, β-actin-containing cytoskeleton. The dense cytoplasmic plaque is localized to TAJs at a location that is analogous to their classical location in the canonical AJC (see diagram in Fig. 7).

Finally, two subdomains are apparent within TAJs and correspond with the segregation of claudins, localization of catenins, differing cytoplasmic plaque densities and recruitment of the cytoskeleton. Together, these characteristics distinguish AJs and TJs from TAJs and highlight the novelty of this hybrid junction.

TAJs are required at DC-OHC junctions

An important question arising from the current study is, why are TAJs assembled at DC-OHC contacts when canonical AJCs suffice at DC-DC interfaces? A simple answer is that prolonged oscillatory strain and shear stresses associated with OHC somatic electromotility and basilar membrane resonance is beyond the limits of canonical AJC function. Hydrodynamic shearing forces on polarized endothelial cell monolayers trigger loss of β-catenin from AJCs, cytoskeleton remodeling and cell shape changes through MAPK signaling (Langille, 2001). In the face of constant shear forces in the organ of Corti, DC-OHC contacts must maintain adhesion to ensure consistent shape, stiffness and integrity of the reticular lamina.

Mechanisms that contribute to DC-OHC junction integrity are not limited to the actin cytoskeleton underlying TAJs, but also include their dovetail shape, which is apparent in Fig. 1g. Thus, the circumference of OHCs gradually decreases from the apical surface to an inflexion point midway through the junction, forming a negative angle with the plane of the reticular lamina, then steadily increases (positive angle) to the bottom of the TAJ. Accordingly, OHC vertical oscillatory motions push and pull against oblique surfaces of the DC-OHC interface, which maximizes mechanical support for these movements.

Implications of TAJs for intercellular junction biology

Genetic studies in *C. elegans* have identified key components of nematode apical junctions, including: HMR-1 (cadherin),

HMP-2 (β-catenin), HMP-1 (α-catenin), JAC-1 (p120^{ctn}) and VAB-9 (a claudin-like protein) in a functional complex that recruits an actin cytoskeleton (Cox and Hardin, 2004; Tepass, 2003). In light of the colocalization of these components, our data suggest evolutionary conservation of occluding-adhesive junctions from invertebrates to mammals.

Importantly, mammalian TAJs appear to have dispensed with cadherins for recruiting catenins to the membrane and it is tempting to speculate that the carboxyl-termini of claudin-9 and -6 contain catenin-binding motifs. However, an intermediary adapter molecule seems more likely because our yeast two-hybrid studies do not reveal claudin-catenin interactions (unpublished data). Furthermore, this adapter may require strand formation for catenin recruitment because claudin-9 and -6 are widely distributed in the plasmalemma of transfected COS-7 cells but only recruit catenins to sites of TJ formation. The ZO-1 protein is an excellent candidate for this adapter because it is recruited to tight and adherens junctions and has been shown to interact with α-catenin (Itoh et al., 1999; Itoh et al., 1993). Indeed, our data are consistent with this possibility.

Our novel findings in mammals, that TAJs mediate recruitment of AJ regulatory proteins, that TAJs assemble an extensive actin cytoskeleton for adhesion and that claudins segregate into subdomains in vivo has significant implications for textbook accounts of intercellular junction identity and function (Fig. 7). The hallmark molecules, catenins and claudins, can no longer be considered as archetypal constituents confined to their respective junctions but rather should be considered mix-and-match modules recruited to membrane specializations to bestow adhesive and/or occluding properties. Furthermore, our data raise the possibility that TAJs are subject to some forms of regulation extensively characterized in AJs, including tyrosine kinase phosphorylation of p120^{ctn}, rho GTPase-mediated cytoskeletal remodeling and β-catenin-mediated transcriptional changes that may be critical to maintaining the integrity of the reticular lamina in the face of acute or chronic hair cell degeneration over the life span of the organism (Anastasiadis and Reynolds, 2001; Harris and Peifer, 2005; Nelson and Nusse, 2004; Peifer and Yap, 2003).

Materials and Methods

Antibodies and general reagents

Antibodies are diluted to 1-2 μg ml^{-1} and obtained from: E-, N- and P-cadherin, β-catenin, p120^{ctn} (Transduction Lab., Lexington, KY), and α-catenin (Becton Dickinson, San Jose, CA). Anti-claudin antibodies are affinity-purified from serum from rabbits immunized with peptide-KLH conjugates (Princeton Biomol., Langhome, PA) matching the carboxyl-terminal sequences of mouse claudin-6 (rabbit serum PB174; peptide sequence, SSGGTQGPRHYMAC), claudin-9 (rabbit serum PB209; peptide sequence, PRGPRLGYSIPSRSGA) and claudin-14 (rabbit serum PB196; peptide sequence, QEEAPYRPYPPQSR; and rabbit serum PB321, peptide sequence CATAPAYRPAAYKDNRA). The immunoreactivity and selectivity of each antibody was tested in COS-7 cells transfected with the corresponding of GFP-claudin fusion protein expression plasmids (supplementary material Fig. S3). Rhodamine-phalloidin, anti-rabbit and anti-mouse secondary antibodies and ProLong antifade mounting media are from Molecular Probes (Eugene, OR). 5-10 nm gold-conjugated anti-mouse and anti-rabbit antibodies are from Amersham (Piscataway, NJ). Bovine serum albumin (BSA) is from Roche (Indianapolis, IN).

Whole-mount organ of Corti preparations and immunocytochemistry

Tympanic bullae are dissected from CO_2-narcotized, decapitated rats, mice and pigmented guinea pigs in accordance with NIH animal use protocol, 1067/02. All data have been generated from adult animals (2-4 months of age) except for supplementary material Fig. S1, for which 6-day-old rats have been used. After removing the bony shell at the apical turn, cochleae are immersed in 4% paraformaldehyde phosphate buffered saline, pH 7.4, (PBS) for 1 hour at RT and perfused through the round and oval windows. For differential-interference contrast imaging, the tectorial membrane is dissected to reveal the organ of Corti and images of the reticular lamina are captured using a 40× oil immersion lens attached to a Nikon microscope. DC-DC and DC-OHC junctions are visible in these preparations and their relative lengths are determined by tracing each junction with a digitizing tablet and OpenLab software (Improvision Ltd, Coventry, UK).

For immunocytochemistry, whole-mount organs of Corti are dissected in PBS, permeabilized for 30 minutes with 0.5% Triton X-100 in PBS, washed in PBS, blocked with 4% BSA for 1 hour, incubated with primary antibodies in 4% BSA for 1 hour, washed in PBS, incubated with FITC-conjugated secondary antibodies in 4% BSA for 30 minutes, counterstained with rhodamine phalloidin for 30 minutes, washed in PBS, mounted in ProLong, and viewed with a Zeiss or with a Nipkow (spinning disc) confocal microscope.

Tissue preparation for electron microscopy

Tissues from adult rats, mice and guinea pigs dissected as described above are fixed with 4% formaldehyde, 0.5% glutaraldehyde, 3 mM $CaCl_2$ in 0.1 M sodium cacodylate buffer, pH 7.2, glycerinated, plunge-frozen in liquid Freon 22, and transferred to liquid nitrogen. Frozen samples are freeze substituted in 1.5% uranyl acetate in 100% methanol at –90°C, infiltrated with Lowicryl HM-20 at –45°C, polymerized with UV light, and immunogold labeled. Freeze-fracture and freeze-etching replicas and the samples processed using the reduced osmium protocol are prepared as described (Kachar et al., 2000; Mammano et al., 1999). Thin sections and replicas are photographed with a Leo 922 Electron Microscope. Fig. 1d and Fig. 6a were filtered using the unsharp mask in Photoshop 7.0 to increase contrast for reproduction. For scanning electron microscopy, tissues are prepared as described (Kachar et al., 2000), and viewed with a Hitachi 4500 Microscope.

Generation of GFP-claudin fusion protein expression plasmids

The cDNAs encoding claudin-9, -6, -11 and -14 were amplified from a mouse organ of Corti expression library (Pompeia et al., 2004). The primer sequences used are: claudin-6, 5′-gtgac*gaattc*t ATG GCC TCT ACT GGT CTG-3′ (sense) 5′-caaa*gtcgac* CAC ATA ATT CTT GGT GGG ATA TTC-3′ (antisense); claudin-9, 5′-actgta*agatct* ATG GCT TCC ACT GGC CTT-3′ (sense) 5′-ggaatc*gtcgac* CAC ATA GTC CCT CTT ATC-3′ (antisense); claudin-11, 5′-gccgtt*gaattc* ATG GTA GCC ACT TGC CTT CAG–3′ (sense) 5′-ggactc*gtcgac* TTA GAC ATG GGC ACT CTT GGC-3′ (antisense); claudin-14, 5′-actgta*gaattc* ATG GCC AGC ACA GCG GTC–3′ (sense) 5′-gaggtc*gtcgac* CAC GTA GTC TAA CAG CCT-3′ (antisense). Italicized nucleotides show restriction sites for cloning into pGFP-C2 (Clontech, Mountain View, CA), which fuse EGFP in-frame with the N-terminus of each claudin. This cloning strategy results in the addition of short peptides to the N- and C-termini of each claudin. At the N-terminus following EGFP, the 12 amino acid peptide is: GRTQISSSSFEF. At the C-terminus, the 13mer is: VDGTAGPGSTGSR. Plasmids are purified (Qiagen maxipreps, Valencia, CA) and bidirectionally-sequenced across the GFP-claudin fusion junction.

Cell transfection and immunofluorescence

COS-7 cells are plated on coverslips at 2×10^5 cells per well (35 mm) and cultured in 10% FBS, GlutaMAX in DMEM (Invitrogen). Cells are transfected with GFP-claudin plasmids or vector control (0.5 μg DNA ml^{-1}) using Gene Juice (Novagen, San Diego, CA). At 24 hours, cells are rinsed with PBS, fixed in –20°C methanol for 5 minutes or 4% paraformaldehyde in PBS for 30 minutes, washed in PBS, incubated in 0.5% Triton X-100 for 10 minutes, washed in PBS, blocked in 4% BSA for 1 hour, incubated in primary antibodies in 4% BSA for 1 hour, washed in PBS and labeled with secondary antibodies.

We thank Gavin P. Riordan, Decio S. Pinto, Cynthia Sterkenburg, Valerie Dodane, and Celine Pompeia (NIH-NIDCD) for help with the early experiments of this study, and Kuni Iwasa and Ronald Petralia (NIH-NIDCD) for comments on the manuscript. This work was supported by NIDCD-IRP, a scholarship to H.W.L. from the Howard Hughes Medical Institute and by grants to A.G. from (NIH-NIDCD, R01-DC006262).

References

Aijaz, S., Balda, M. S. and Matter, K. (2006). Tight junctions: molecular architecture and function. *Int. Rev. Cytol.* **248**, 261-298.

Anastasiadis, P. Z. and Reynolds, A. B. (2001). Regulation of Rho GTPases by p120-catenin. *Curr. Opin. Cell Biol.* **13**, 604-610.

Ben-Yosef, T., Belyantseva, I. A., Saunders, T. L., Hughes, E. D., Kawamoto, K., Van Itallie, C. M., Beyer, L. A., Halsey, K., Gardner, D. J., Wilcox, E. R. et al. (2003). Claudin 14 knockout mice, a model for autosomal recessive deafness DFNB29, are deaf due to cochlear hair cell degeneration. *Hum. Mol. Genet.* **12**, 2049-2061.

Cox, E. A. and Hardin, J. (2004). Sticky worms: adhesion complexes in C. elegans. *J. Cell Sci.* **117**, 1885-1897.
Farquhar, M. G. and Palade, G. E. (1963). Junctional complexes in various epithelia. *J. Cell Biol.* **17**, 375-412.
Furuse, M., Sasaki, H., Fujimoto, K. and Tsukita, S. (1998). A single gene product, claudin-1 or -2, reconstitutes tight junction strands and recruits occludin in fibroblasts. *J. Cell Biol.* **143**, 391-401.
Furuse, M., Sasaki, H. and Tsukita, S. (1999). Manner of interaction of heterogeneous claudin species within and between tight junction strands. *J. Cell Biol.* **147**, 891-903.
Gow, A., Southwood, C. M., Li, J. S., Pariali, M., Riordan, G. P., Brodie, S. E., Danias, J., Bronstein, J. M., Kachar, B. and Lazzarini, R. A. (1999). CNS myelin and sertoli cell tight junction strands are absent in *Osp/Claudin 11*-null mice. *Cell* **99**, 649-659.
Gulley, R. L. and Reese, T. S. (1976). Intercellular junctions in the reticular lamina of the organ of Corti. *J. Neurocytol.* **5**, 479-507.
Gumbiner, B. M. (2005). Regulation of cadherin-mediated adhesion in morphogenesis. *Nat. Rev. Mol. Cell Biol.* **6**, 622-634.
Harris, T. J. and Peifer, M. (2005). Decisions, decisions: beta-catenin chooses between adhesion and transcription. *Trends Cell Biol.* **15**, 234-237.
Itoh, M., Nagafuchi, A., Yonemura, S., Kitani-Yasuda, T. and Tsukita, S. (1993). The 220-kD protein colocalizing with cadherins in non-epithelial cells is identical to ZO-1, a tight junction-associated protein in epithelial cells: cDNA cloning and immunoelectron microscopy. *J. Cell Biol.* **121**, 491-502.
Itoh, M., Morita, K. and Tsukita, S. (1999). Characterization of ZO-2 as a MAGUK family member associated with tight as well as adherens junctions with a binding affinity to occludin and alpha catenin. *J. Biol. Chem.* **274**, 5981-5986.
Jahnke, K. (1975). The fine structure of freeze-fractured intercellular junctions in the guinea pig inner ear. *Acta Otolaryngol. Suppl.* **336**, 1-40.
Kachar, B., Parakkal, M., Kurc, M., Zhao, Y. and Gillespie, P. G. (2000). High-resolution structure of hair-cell tip links. *Proc. Natl. Acad. Sci. USA* **97**, 13336-13341.
Kitajiri, S., Furuse, M., Morita, K., Saishin-Kiuchi, Y., Kido, H., Ito, J. and Tsukita, S. (2004). Expression patterns of claudins, tight junction adhesion molecules, in the inner ear. *Hear. Res.* **187**, 25-34.
Kobielak, A., Pasolli, H. A. and Fuchs, E. (2004). Mammalian formin-1 participates in adherens junctions and polymerization of linear actin cables. *Nat. Cell Biol.* **6**, 21-30.
Langille, B. L. (2001). Morphologic responses of endothelium to shear stress: reorganization of the adherens junction. *Microcirculation* **8**, 195-206.
Mammano, F., Frolenkov, G. I., Lagostena, L., Belyantseva, I. A., Kurc, M., Dodane, V., Colavita, A. and Kachar, B. (1999). ATP-Induced Ca(2+) release in cochlear outer hair cells: localization of an inositol triphosphate-gated Ca(2+) store to the base of the sensory hair bundle. *J. Neurosci.* **19**, 6918-6929.
Nagafuchi, A. (2001). Molecular architecture of adherens junctions. *Curr. Opin. Cell Biol.* **13**, 600-603.
Nelson, W. J. and Nusse, R. (2004). Convergence of Wnt, beta-catenin, and cadherin pathways. *Science* **303**, 1483-1487.
Ospeck, M., Dong, X. X. and Iwasa, K. H. (2003). Limiting frequency of the cochlear amplifier based on electromotility of outer hair cells. *Biophys. J.* **84**, 739-749.
Peifer, M. and Yap, A. S. (2003). Traffic control: p120-catenin acts as a gatekeeper to control the fate of classical cadherins in mammalian cells. *J. Cell Biol.* **163**, 437-440.
Pompeia, C., Hurle, B., Belyantseva, I. A., Noben-Trauth, K., Beisel, K., Gao, J., Buchoff, P., Wistow, G. and Kachar, B. (2004). Gene expression profile of the mouse organ of Corti at the onset of hearing. *Genomics* **83**, 1000-1011.
Schneeberger, E. E. and Lynch, R. D. (2004). The tight junction: a multifunctional complex. *Am. J. Physiol. Cell Physiol.* **286**, C1213-C1228.
Simske, J. S., Koppen, M., Sims, P., Hodgkin, J., Yonkof, A. and Hardin, J. (2003). The cell junction protein VAB-9 regulates adhesion and epidermal morphology in C. elegans. *Nat. Cell Biol.* **5**, 619-625.
Tepass, U. (2003). Claudin complexities at the apical junctional complex. *Nat. Cell Biol.* **5**, 595-597.
Tsukita, S., Furuse, M. and Itoh, M. (2001). Multifunctional strands in tight junctions. *Nat. Rev. Mol. Cell Biol.* **2**, 285-293.
Wangemann, P., Liu, J. and Marcus, D. C. (1995). Ion transport mechanisms responsible for K+ secretion and the transepithelial voltage across marginal cells of stria vascularis in vitro. *Hear. Res.* **84**, 19-29.
Wilcox, E. R., Burton, Q. L., Naz, S., Riazuddin, S., Smith, T. N., Ploplis, B., Belyantseva, I., Ben-Yosef, T., Liburd, N. A., Morell, R. J. et al. (2001). Mutations in the gene encoding tight junction claudin-14 cause autosomal recessive deafness DFNB29. *Cell* **104**, 165-172.
Zigmond, S. (2004). Formin' adherens junctions. *Nat. Cell Biol.* **6**, 12-14.

Journal of Cell Science